Degradation from Tartrazine Dye Yellow in Solvent Solution via SnO_2 NPs

Saad Khalaf Madlool [1]
[1] Department of Physics, College of Science, Mustansiriyah University, Baghdad, Iraq
E-mail: saadkhalaf79@yahoo.com

[1] Waafa Mahdi Salih
[1] Department of Physics, College of Science, Mustansiriyah University, Baghdad, Iraq
Waafaamsalkhayat@yahoo.com

Ahmed Mahdi Rheima[2]
[2] Department of Chemistry, College of Science, Mustansiriyah University, Baghdad, Iraq
ahmed.rheima@gmail.com

ABSTRACT

Simple chemical method was used to create tin oxide nanoparticles (SnO_2 NPs), which were then annealed at various temperatures for characterisation. X-ray diffraction, scanning electron microscopy, and optical spectroscopy were used to analyze the powders. Due to their low cost, appropriate stability qualities, strong photosensitivity, etc., tin oxide (SnO_2) nanoparticles are of tremendous interest in various sectors, including catalytic, electrochemical, and biological applications. The type of transition and band gap of the produced nanoparticles were calculated from the absorption spectra. The optical UV-visible spectrum displays a clearly defined absorption that is significantly blue-shifted in relation to the peak absorption of bulk SnO_2, suggesting the impact of quantum size.

Keywords: SnO_2 NPs; Simple chemical method; photosensitivity; green synthesis

1. Introduction

Due to their fascinating (unique electrical, physical, chemical, and magnetic) properties that differ from those of their corresponding bulk form, nanomaterials have received a lot of attention. In studies relating to their underlying mechanism, such as the size effect and the quantum effect, as well as towards the use of these materials, enormous efforts are being made towards the development of nanoscale sized materials. The semiconductor's band structure changes as particle size decreases; the band gap widens and the margins of the bands break into distinct energy levels. These 'quantum scale effects' do exist [1-11]. Tin oxides are made using a variety of techniques, such as thermal evaporation of oxides, quick oxidation of pure tin, chemical vapor deposition CVD spray pyrolysis, and air-evaporation of tin grains. The cassiterite structure of SnO2 [12-15]. Metal oxide semiconductors are an affordable and reliable gas sensor technology. SnO2 has been garnering a lot of attention among the many metal oxide semiconductors due to its high conductivity, transparency, and gas sensitivity. Out of all the approaches, the co-precipitation method is the easiest, cheapest, and doesn't require high pressure or temperature . By adjusting the pH of the medium, the precursor's concentration, and the precipitating reagents, the size and form of the particle can be adjusted in this approach. Filtration and repeated washing were effective

ways to remove impurities from the precipitate, and eventually the particles started to aggregate. As a result, emphasis has been placed on employing the co-precipitation process to create pure and extremely crystalline SnO_2 nanoparticles.

2. Experimental

2.1. synthesis of tin oxide nanoparticles

Tin chloride ($SnCl_{2.5}H_2O$) was used in the precipitation process to create SnO nanostructures. To create Concentrated solution, each precursor was first dissolved in 50 ml of deionized water. Drop by drop, urea (50ml) is added to the solution. 50 cc of NaOH solution were steadily added while being vigorously stirred until pH reached 14. Precipitates were collected, and deionized water was used to rinse them repeatedly until the pH approached 7. The washed precipitates were then dried at 100 °C for 16 hours repeatedly. The precursors were then calcined for 3 hours at 450 °C. using X-Ray Diffractometer (XRD) analysis.

2.2. Adsorption of Tartarazine dye yellow on Tin oxide surface

Adsorption is a tried-and-true but effective method for removing organics or heavy metals from aqueous solutions. For the purpose of developing adsorption operations, the equilibrium isotherm of a specific adsorbent serves as a representation of its adsorbent qualities. a standard response to the In deionized water, tartrazine yellow dye (1000 ppm) was produced. 10 ml of dye solution were mixed with 0.001 g of SnO_2 nanoparticles, which were then heated for around 30 minutes at various temperatures of 288 K, 298 K, 308 K, 318 K, and 328 K. A UV-visible absorption spectrophotometer was used to quantify the dye concentration in the filtrate after the solution had been filtered. [16-17].

$$Qe = (C_0 - Ce)Vsol/M \quad (1)$$

Where by Qe (mg/g) denotes the equilibrium adsorption capacity, C and Ce denote the initial and equilibrium concentrations of Tartarazin yellow dye, respectively, and M denotes the mass of the SnO nanoparticles (g). Tartarazin yellow's volume is thus designated as V sol.

2.3 Characterization

The PANalytical X'Pert X-ray diffractometer was used to identify the phase and determine the size of the crystallite (CuK_ target, = 0.154nm). Data from XRD were gathered in employing step scan mode, step width of 0.020, and step time of 2.40 s, in the 2 range of 20-800. Model Jeol JSM6010LV field emission scanning electron microscope A 300-mesh Sn grid was covered with a total of 20 L, which was then allowed to dry at ambient temperature. To determine the emission's energy gap, SnO2 nanoparticles' photoluminescence (PL) emission was monitored. With a 5kV accelerating violation, the TEM model Jeol JSM-6010LV detected sample morphologies at magnifications of 500 X and 60 kX.For around 15 minutes[18-19], TEM studies the sample SnO2 nanoparticle powder discrete in the deionized and sonic water.

3. Results and Discussion

3.1. XRD analysis

The generated SnO_2 nanoparticles' X-ray diffraction pattern, which is shown in Figure 1, confirms that they are polycrystalline. The earlier researchers [20] found similar X-ray diffractograms for SnO2 nanoparticles made in various ways. Diffraction angles and line intensity were more precisely quantified using the diffraction profile. The JCPDS file of SnO_2 (JCPDS 41-1445) reports the expected peaks (110) (101) and (211) as the identifying peaks for SnO_2 nanoparticles. It has been determined from the diffraction profile that The synthesized SnO_2 nanoparticles have a tetragonal, polycrystalline structure with a preferred orientation along the (110) plane. The peak (110) experiences a markedly faster increase in intensity than the other peaks. Utilizing the relation, the lattice parameters 'a' and 'c' for the tetragonal-shaped SnO_2 nanoparticles were evaluated.

Using Debye Scherrer's formula, the crystallite size (D) of the SnO2 nanoparticles was calculated.

$D=0.9\lambda/\beta cos\theta$

(2)

where is the whole width at half maximum (FEHM) of the corresponding peak of the XRD pattern and is the wavelength of the radiation source (CuK). The aforementioned relation was used to compute the lattice constants from the observed 'd' spacing, (hkl) planes, and the results are in good agreement. Between 20 nm and 27 nm is the range for the average crystallite size (D) calculated from the XRD spectra using Scherer's formula.

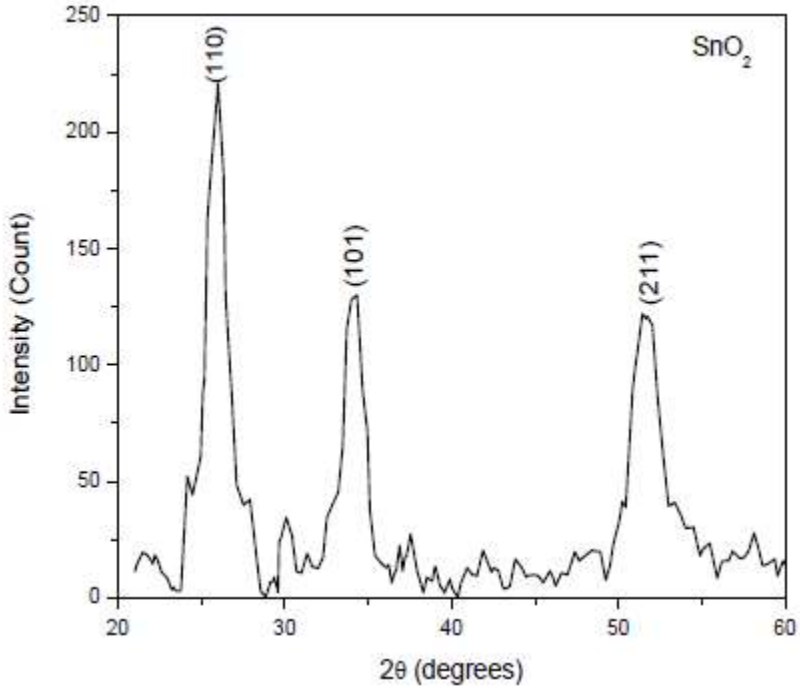

Figure1. XRD diffractogram of SnO_2 nanoparticles.

3.2. TEM analysis

Figure 2 displays a TEM image of nanoparticles in various sizes and shapes. The particles ranged in size from 25 nm, with an average size of 29.7 nm. The aggregation of smaller nanoparticles into larger particles may have dimensions that match those found in the XRD study. Due to the large number of parallel lattice surfaces inducing diffraction, XRD measurements of crystallite size are reliant on the expansion of Bragg's reflections. Although the size distribution is not taken into account, the Scherrer equation parameter k approximates the crystallite shape factor, leading to size figures that are different from the TEM.

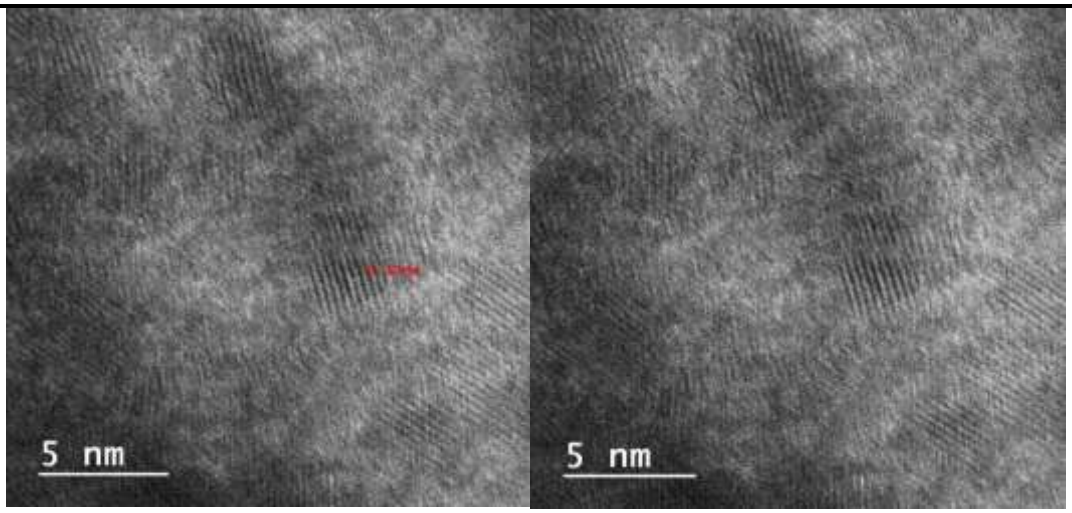

Figure 2. TEM analysis of SnO_2 nanoparticles.

3.3. SEM characterization

The form and growth characteristics of aggregates of the as-prepared SnO_2 nanoparticles were examined using scanning electron microscopy (SEM) at various magnifications. SnO_2 particles with nanoscale dimensions are interconnected in Figure 3 (a, b), which demonstrates substantial agglomeration along with numerous small spherically shaped particles. Actually, this agglomeration is made up of much larger grains that are between 100 and 200 nm in size .The relative rates of the nucleation and growth processes, as well as the degree of agglomeration, largely determine the particle size and dispersion of nanoparticles. It is interesting to note that SnO2 particles are small and can aggregate with other finer particles to create larger clusters as magnification increases. The particle size and dispersion of nanoparticles are mostly determined by the relative speeds of the nucleation and growth processes, as well as the degree of agglomeration. It's interesting to observe that although SnO_2 particles are small, as magnification increases, they can join forces with other, smaller particles to form larger clusters.

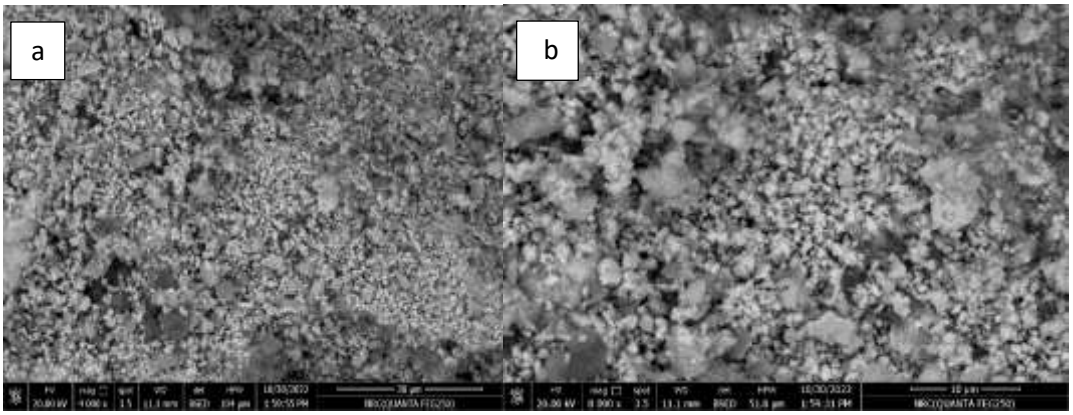

Figure 3. SEM micrographs of the SnO_2 nanoparticles.

3.4. EDX characterization

Figure 4 displays the EDX spectrum of SnO nanoparticles. The EDS technique is used to determine whether there are tin particles in the tin oxide produced sample. SnO2 has been measured using a SEM (JSM-6510, SAI Labs, TIET Patiala) on a scale of 0 to 14 KeV

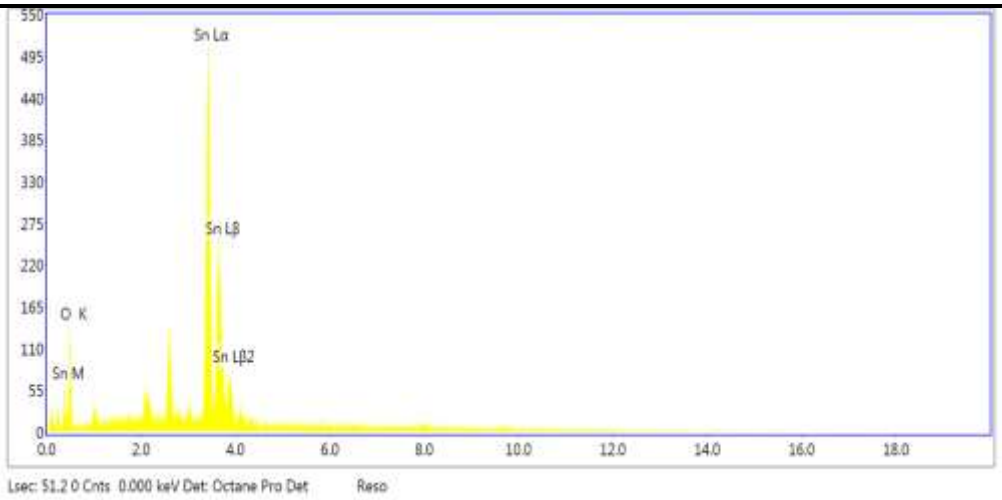

Figure 4. EDX spectrum of SnO_2 NPs.

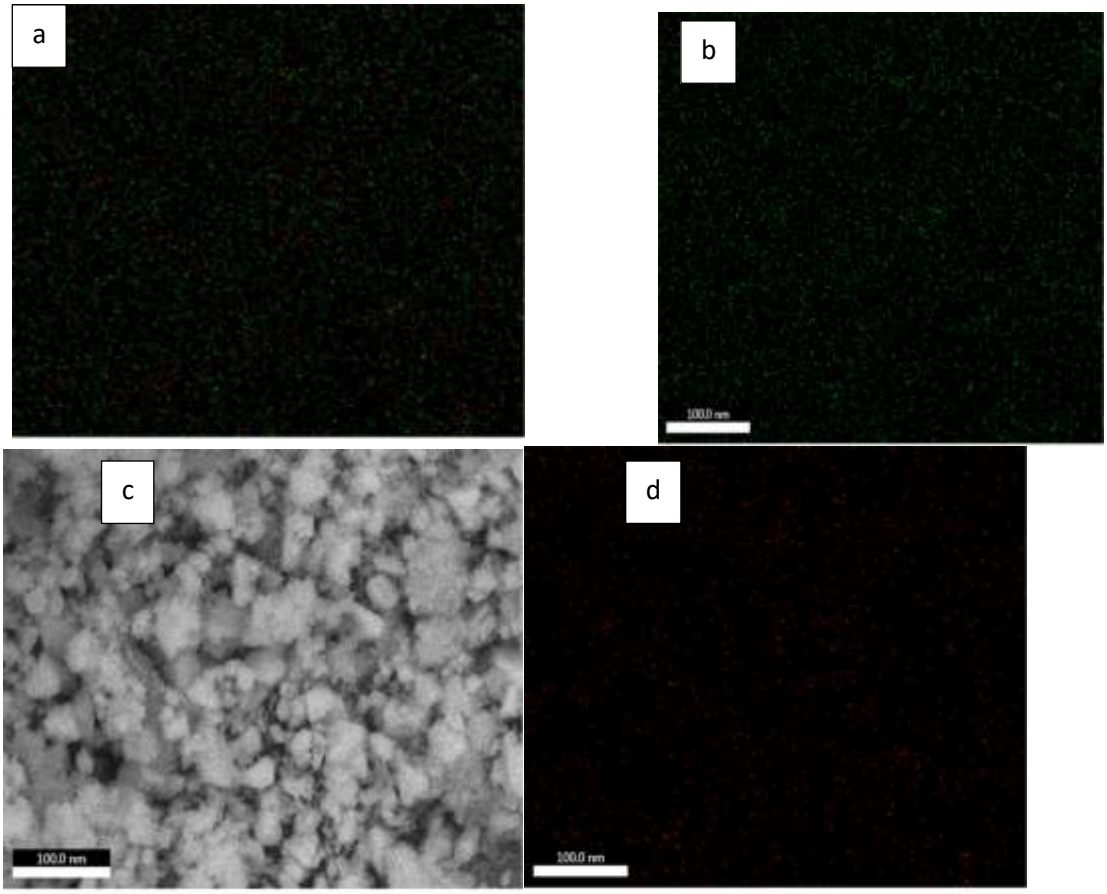

Figure 5 (a-d). X-ray mapping of SnO_2 NPs

Adsorption isotherms

Adjusting the adsorption isotherm to the adsorption results to determine how the dye and adsorption interact is the primary step in the adsorption analysis. In this paper, the Freundlich and Langmuir models were taken into account. The linear Freundlich adsorption process is shown in the formula below [21]:

$$\log(Qe)=\log(kf)+(1n)\log(Ce) \quad (3)$$

The adsorption capacity and adsorption intensity are represented by the so-called Freundlich constants Kf and n, respectively.

According to Figure 7, The kf and n are calculated from the intercept and slope, respectively (0.832). This outcome is in line with the physically verified adsorption [22]. The Freundlich isotherm model better describes the adsorption (R2 = 0.8903).

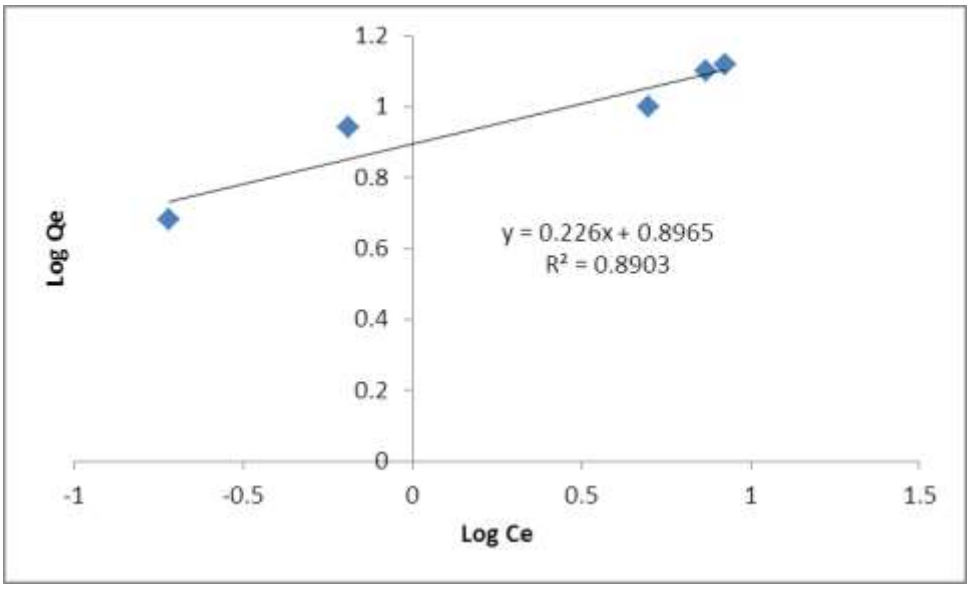

Figure 7: the frendlesh isotherm model at 298 k.

The following formulation demonstrates how the data complies with the Langmuir adsorption isotherm: [23]:

$$Ce/Qe=1/(qmax)\ Kl+ Ce/(qmax) \quad (4)$$

The Langmuir constant (KL) is measured in mg/L, while the maximum amount of Tartarazin yellow dye (q max) is measured in mg/g. The separation factor that shows and refers to the dimensionless constant (RL).

$$Rl= 1/(1+KlCi) \quad (5)$$

Effect of contact time

In a series of tests, contact time and equilibrium time were measured using 0,01 g of SnO_2 NPs in 10 mL of dye (10 ppm). The mixture was shaken at 298 K at 185 rpm. The first 30-45 minutes, adsorption happens quite swiftly. The tight connection between the active SnO_2 nanoparticles and the dye is what causes the quick adsorption. After 30 minutes, as demonstrated in Figure 8, the dye's adsorption rate stabilizes due to the nanoparticles' surface.

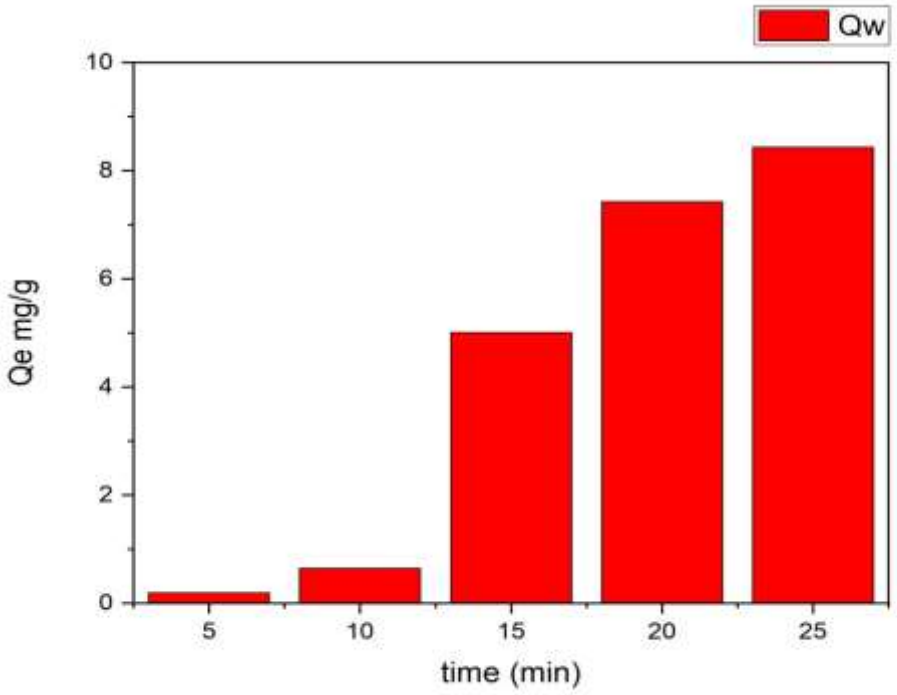

Figure 8. Effect of time on adsorption of dye onto the SnO_2 NPs.

Effect of adsorbent mass

The effectiveness of the adsorbent was established by adding different amounts of SnO_2 NPs to 10 ppm of dye (0.01 g, 0.05 g, 0.1 g, and 0.15 g). The mixture was shaken at 298 K at 185 rpm. The graph illustrates the association between mass and the quantity of adsorption. First, the adsorption speed is extremely fast in nanocomposites because of the increase in active sites. Figure 10 demonstrates the increase in dye adsorption. through an increase in the bulk of SnO_2 NPs.

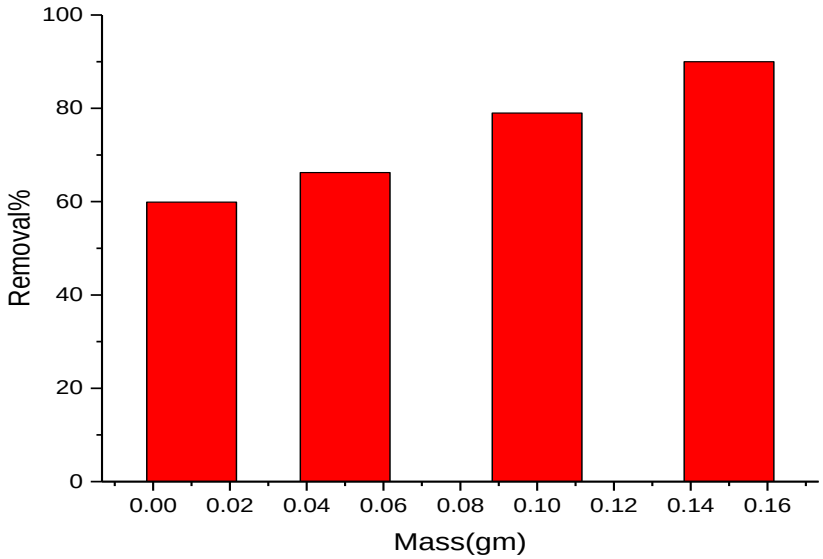

Figure.10 Effect of adsorbent mass on adsorption of dye onto the SnO_2 NPs.

Effect of Temperature

At specific temperatures of 288 K, 298 K, 308 K, 318 K, and 328 K, the temperature

influence of dye adsorption on the SnO_2 NP surface was investigated [27,28]. The amount of dye adsorption solution grows as the temperature rises. The endothermic process is the result, and the average value of ΔH° is positive. This illustrates how absorption and adsorption work. The rate of diffusion increases as a function of temperature, the diffusion molecules are absorbed in the holes, and the adsorbent and the strong link are all connected. Thermodynamic parameters offer precise information on changes in the inherent energy caused by adsorption, therefore they should be examined appropriately. In this analysis, the free energy of adsorption (ΔG°), entropy (ΔS°), and enthalpy (ΔH°) were utilized to quantify the following adjustments in order to anticipate the mechanism of adsorption [23-28]:

$$\ln(Ke) = -\Delta H\, RT + \Delta S\, R \quad (6)$$

$$Ke = Qe/Ce \quad (7)$$

$$\Delta G = \Delta H \_ T\Delta S \quad (8)$$

Ke is the equilibrium constant, R is the gas constant (8.314 J/mol K), and T is the temperature in Kelvin (K). Figure 11 shows a van't Hoff plot between ln K and 1/T. The reaction was endothermic, as evidenced by the ΔH, which was 7.630514 kJ/mole determent by slope. The intercept's ΔS value of 20.8 J/mole indicated that the adsorbed particles were still moving steadily on the surface. Both absorption and adsorption applied. 1.415 KJ/mole at 298 K, the positive Δ G value, indicates non-spontaneous adsorption

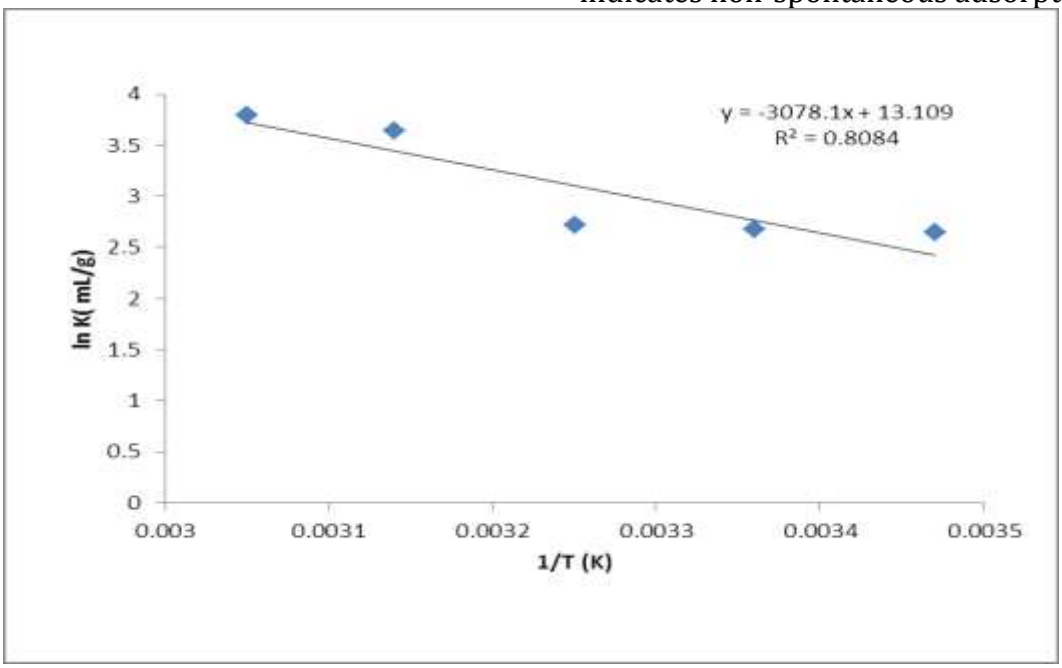

Figure 11. the van't Hoff plot between ln K and 1/T.

4. Conclusions

Simple chemical method has been used to create SnO_2 nanoparticles. The tetragonal crystalline structure of the SnO_2 nanoparticles was confirmed by the XRD investigation. Simple chemical method of SnO_2 nanoparticles has the potential to provide a wide range of optoelectronic devices and solar cell applications. A number of characterizations were used to describe the synthetic tin oxide, including FTIR, XRD, SEM, EDAX, and UV-Vis. The XRD technique was used to study the structural characteristics. Chemical precipitation has been used to successfully create pure SnO_2 core-shell nanoparticles. X-ray diffraction investigation confirmed that pure SnO_2 had a tetragonal structure. The creation of core-shell structures and spherical shape are both confirmed by TEM micrographs. FT-IR spectra were used to determine whether the substance contained any elementary particles. However, more research is required to determine whether the preferred optical properties make some materials a preferable choice for optoelectronic devices.

References

1. Sucharita Ch., Mouni R., Rajnarayan S., (2020), Cost-effective synthesis method of facile environment friendly SnO2 nanoparticle for efficient photocatalytic degradation of water contaminating compound. Water Sci. Technol. 81: 508–517.
2. Nasir Z., Shakir M., Wahab R., Shoeb M., Alam P., Hasan Khan R., Mobin M., Lutfullah M., (2017), Co-precipitationsynthesis and characterization of Co doped SnO2 NPs, HAS interaction via various spectroscopic techniques and their antimicrobial and photocatalytic activities. Int. J. Biolog. Macromolec. Part A. 94: 554-565.
3. Ahmad Khan Sh., Kanwal S., Rizwan K., Shahid S., (2018), Enhanced antimicrobial, antioxidant, in vivo antitumor and in vitro anticancer effects against breast cancer cell line by green synthesized un-doped SnO2 and Co-doped SnO2 nanoparticles from Clerodendrum inerme. Microbial Pathogenesis. 125: 366-384.
4. Kim Y., Yang S., Kang Y., Kim B. K., Lee H., (2018), Transition metal doped Sb@SnO2 nanoparticles for photochemical and electrochemical oxidation of cysteine. Scient. Reports. 8: 12348-12352.
5. Karmaoui M., Belen Jorge A., McMillan P. F., Abil E., Aliev F.,Pullar R. C., António Labrincha J., Maria Tobaldi D., (2018), One-step synthesis, structure, and band gap properties of SnO2 nanoparticles made by a low temperature nonaqueous sol–gel technique. ACS Omega. 3: 13227–13238.
6. Suresh G., Sathishkumar R., Iruson B., Sathyaseelan B.,Senthilnathan K., Manikandan E., (2019), Study on structural,luminescence properties and Hall Effect of SnO2 nanoparticles obtained by a Co-precipitation technique. Int. J. Nano Dimens. 10: 242-251.
7. Hyo-Jin A., Hyun-Chul Ch., Kyung-Won P., Seung-Bin K., Yung-Eun S., (2004), Investigation of the structural and electrochemical properties of size-controlled SnO2 nanoparticles. J. Phys. Chem. B. 108: 9815-9820.
8. Feng G.., Shu Fen W., Meng Kai L., Yong Xin Q., Guang J. Zh., Dong X., Duo Rong Y., (2003), Preparation and luminescence characteristics of nanocrystalline SnO2 particles doped with Dy3+. J. Crystal Growth. 255: 357–360.
9. Paulo Mendes G., Mario Moreira L., Sergio M. T., Marcelo O. O., Andres J., Maximu L. S., Diaz-Mora N., Jose Varela A., Elson L., (2012), SnO2 nanocrystals synthesized by microwave-assisted hydrothermal method: Towards a relationship between structural and optical properties. J. Nanopart. Res. 14: 750-758.
10. Feng G., Shu Fen W., Chun Feng S., Meng Kai L., Yong Xin Q., Guang Jun Z., Dong X., Duo Rong Y., (2003), Synthesis and luminescence properties of SnO2 nanoparticles. Chem. Phys. Lett. 372: 451–454.
11. Shah D. G., Trivedi P. M., (2012), Preparation, characterizationof nanometer SnO2. Pelagia Res. Lib. Der Chemica Sinica. 3: 1002- 1008.
12. Patil GE, Kajale DD, Gaikwad VB and Jain GH. Preparation and characterization of sno2 nanoparticles by hydrothermal route (2012) Int Nano Lett 2: 17. https://doi.org/10.1186/2228-5326-2-17
13. Zhang J and Gao L. Synthesis and characterization of nanocrystalline tin oxide by sol-gel method (2004) J Solid State Chem 177: 1425-1430.
14. Zhu H, Yang D, Yu G, Zhang H and Yao K. A simple hydrothermal route for synthesizing SnO2 quantum dots (2006) Nanotechnology 17: 2386-2389 .
15. Kumar V, Singh K, Sharma J, Kumar A, Vij A et al. Zn-doped sno2 nanostructures: structural, morphological and spectroscopic

properties (2017) J Mater Sci Mater Electron 28: 18849-18856.
16. Rheima A, Anber AA, Shakir A, Salah Hammed A, Hameed S. Novel method to synthesis nickel oxide nanoparticles for antibacterial activity. *Iran. J. Phys. Res.*, 2020, 20(3), 51-55.
17. Mohammed MA, Rheima AM, Jaber SH, Hameed SA. The removal of zinc ions from their aqueous solutions by Cr_2O_3 nanoparticles synthesized via the UV-irradiation method. *Egypt. J. Chem.*, 2020, 63(2), 425-431.
18. Mohammed Ali Dheyab , Azlan Abdul Aziz , Mahmood S. Jameel and Nazila Oladzadabbasabadi , surfaces-and-interfaces, 2022, 101677, Recent advances in synthesis, modification, and potential application of tin oxide nanoparticles
19. P. Parameswari and A. Sakthivelu , BioNanoScience , pages1211–1219 (2022), Microwave-Assisted Green Process of Cobalt Ferrous Codoped Tin Oxide Nanoparticles: Antibacterial, Anticancer, and Toxicity Performance .
20. Sucharita Ch., Mouni R.and Rajnarayan S., (2020), Cost-effective synthesis method of facile environment friendly SnO2 nanoparticle for efficient photocatalytic degradation of water contaminating compound. Water Sci. Technol. 81:508–517.
21. Safri, A., Fletcher, A.J., Abdel-Halim, E., Ismail, M.A. and Hashem, A., 2020. Calligonum crinitum as a novel sorbent for sorption of Pb (II) from aqueous solutions: thermodynamics, kinetics, and isotherms. Journal of Polymers and the Environment, pp.1-11.
22. Lima, E.C., Gomes, A.A. and Tran, H.N., 2020. Comparison of the nonlinear and linear forms of the van't Hoff equation for calculation of adsorption thermodynamic parameters (Δ S° andΔ H°). Journal of Molecular Liquids, 311, p.113315.
23. Wu, W., Lu, C., Yuan, M., Tian, Y. and Zhou, H., 2021. Acidification of potassium bismuthate for enhanced visible-light photocatalytic degradation ability: an effective strategy for regulating the abilities of adsorption, oxidation, and photocatalysis. Applied Surface Science, p.148873.